Arabian Journal of Chemistry (2016) xxx, xxx–xxx

King Saud University

Arabian Journal of Chemistry

www.ksu.edu.sa
www.sciencedirect.com

ORIGINAL ARTICLE

Chitosan/nano ZnO composite films: Enhanced mechanical, antimicrobial and dielectric properties

P. Mujeeb Rahman [a], V.M. Abdul Mujeeb [a], K. Muraleedharan [a,*], Steni K. Thomas [b]

[a] Department of Chemistry, University of Calicut, Malappuram 673635, India
[b] Department of Life Sciences, University of Calicut, Malappuram 673635, India

Received 8 January 2016; accepted 15 September 2016

KEYWORDS

Chitosan nano ZnO composite film;
Dielectric properties;
Antimicrobial properties;
Antimicrobial packaging material

Abstract For the first time, unfocused Chitosan nano ZnO composite film was prepared by a simple one pot procedure. The novel composite materials were ably characterized by various physicochemical methods. Dielectric and conductivity features of composite materials were analysed. The result showed that both dielectric constant and conductivity values were improved when nano ZnO was incorporated. The potential applicability of composite films to perform as an efficient antimicrobial packaging material was evaluated. Antimicrobial analysis showed that all composite films exhibited enhanced antimicrobial efficacy as compared to pure chitosan film and it is linearly related to the amount of ZnO particles in the matrix.

1. Introduction

The exploitation of biodegradable and environmentally benign Chitosan films has been increased due to the concerns over the environmental issues developed by the disposal of synthetic polymer (Xu et al., 2005). Researchers have greatly focused on Chitosan as an alternative to petroleum derived polymer films owing to its unique properties that are available from renewable sources, biodegradability and the ability to form excellent films (Bourtoom and Chinnan, 2008). Recently, Chitosan films have been fabricated as a protective food packaging material (Martínez-Camacho et al., 2010), but its wide application has been limited owing to inadequate mechanical and antimicrobial properties. The higher water vapour permeability makes the Chitosan film an awful choice for moisture sensitive packaging applications. Hence, further modification of bare Chitosan film is inevitable for the industrial exploitation of this gifted biopolymer. Since, Chitosan is blessed with a very large number of pendant groups such as $-NH_2$ and $-OH$, it can accommodate new functional materials in its matrix paving the way for enhanced properties (Dutta et al., 2009).

In the current scenario of biocomposite research, hybridization of Chitosan with different nano materials has been attracted great attention of researchers. Recently, various types of Chitosan nanocomposites have been synthesized with different types of nanoparticles (Chen et al., 2008; Dehnad et al., 2014; Jiang et al., 2012 , 2009; Tripathi et al., 2011; Zhu et al., 2009). However, till date a few researchers have reported bionanocomposites of Chitosan with Zinc oxide particles. Nano ZnO is a versatile semiconductor material and applied in solar cells, photovoltaic devices, batteries, biosensors and antimicrobial materials (Salehi et al., 2010; Yan et al., 2011; Zhang et al., 2008).

* Corresponding author. Fax: +91 494 2400269.
E-mail address: kmuralika@gmail.com (K. Muraleedharan).
Peer review under responsibility of King Saud University.

ELSEVIER Production and hosting by Elsevier

http://dx.doi.org/10.1016/j.arabjc.2016.09.008

Please cite this article in press as: Mujeeb Rahman, P. et al., Chitosan/nano ZnO composite films: Enhanced mechanical, antimicrobial and dielectric properties. Arabian Journal of Chemistry (2016), http://dx.doi.org/10.1016/j.arabjc.2016.09.008

Aim of the present work was to synthesize Chitosan-nano ZnO films by adopting a simple and one pot procedure, which will contribute to the developments of bionanocomposites and can be used as a potential candidate for antimicrobial packaging purposes as well as dielectric materials. The highlights of this process include utilization of renewable resources, one pot procedure for synthesis and simple sol-cast method to prepare films.

2. Experimental

2.1. Materials

Chitosan with 85 per cent degree of deacetylation was purchased from Sigma Aldrich Co., Ltd (USA). Acetic acid, Sodium hydroxide and Zinc acetate dihydrate were obtained from Merck (Germany). Mineral salt broth and Nutrient agar were purchased from Himedia Chemicals (Mumbai, India). Two bacterial strains Escherichia Coli (*E. coli*, MTCC737) and Staphylococcus Aureus (*S. aureus*, MTCC 1687) were cultured in the Microbiology Laboratory, Department of Life Sciences, University of Calicut. Deionized water was used to prepare all solutions. All the chemicals were analytical grade and used without further purification.

2.2. Preparation of films

Chitosan nano ZnO composite films were prepared by solution casting technique. Two grams of Chitosan flakes was dissolved in 100 mL of 2% (v/v) aqueous acetic acid using ultra sonication for 2 h at room temperature. Subsequently, 2 g zinc acetate dihydrate was added into this solution and the reaction mixture was again sonicated for 1 h to dissolve all zinc acetate molecules. To obtain even films, 25 mL of the viscous mixture was casted in a circular glass dish and dried at room temperature. Glass plates with dried thin films were immersed into 0.2 mol L^{-1} sodium hydroxide solution for wet phase separation. After coagulation, solidified films were kept in a constant temperature oven at 60 ± 0.2 °C for 4 h. The resulting nanocomposite films (C-2) were then washed with methanol for three times, and dried in an oven kept at 60 ± 0.2 °C. Three more nanocomposite films were prepared by adopting same procedure with different quantity of zinc acetate (1.5, 1 and 0.5 g), named as C-1.5, C-1 and C-0.5 (Fig. 1). A pure chitosan film was prepared without zinc acetate and named as C.

2.3. Characterization of films

FT-IR spectra of the films were calibrated using an Attenuated Total Reflection (ATR) Technique (Model, PerkinElmer Inc. USA), and X-ray diffraction (XRD) patterns of samples were obtained in the scanning range of 20–75° by X-ray diffractometer (Model: Rigaku Miniflex 600 diffractometer) with Cu Kα radiation (λ = 0.15406 nm). Thermo gravimetric analysis (TGA) of films was performed (Model: TGA/DTA 851e) to investigate the thermal stability. During the analysis each sample was heated from 25 to 800 °C at a scanning rate of 2 °C min^{-1} under a dynamic nitrogen atmosphere. Surface morphology of samples was observed by scanning electron microscopy (SEM) (Model: Hitachi SU-6600 FESEM), when the measurement samples were sputtered with a layer of gold to prevent the charging effect.

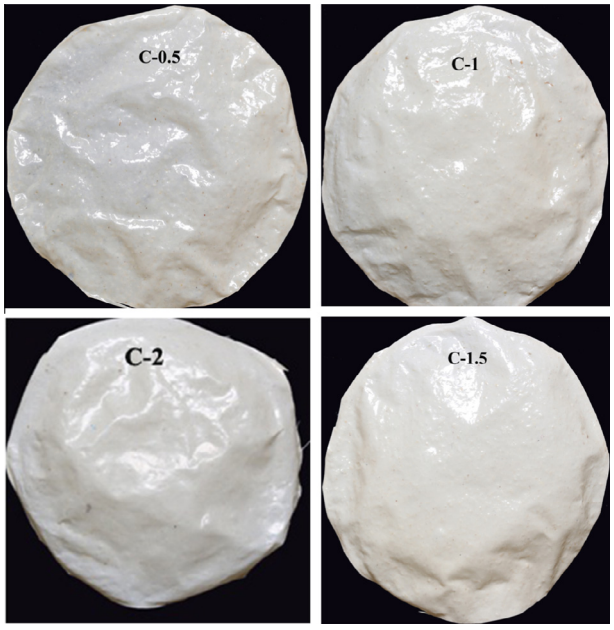

Figure 1 Photographs of prepared nanocomposite films.

2.4. Measurement of mechanical properties

Mechanical properties of films were evaluated by Instron Universal Testing Machine (Model-3345), at a test speed of 1.0 mm/min at room temperature (23–27 °C). Specimens were taken in dumbbell shapes for the analysis. The values of tensile strength (TS) and percentage of elongation at break (%E) were reported as the average of three replicates.

2.5. Water vapour transmission rate

The water vapour transmission rate (WVTR) of films was analysed according to ASTM E96-95 method with required modifications. Circular Plexiglass cups with inner diameter 35 mm and height 45 mm were chosen for the analysis. 25 mL of distilled water was taken in each test cup and cup mouth was sealed perfectly by films having uniform thickness. The distance between water level and the film was 20 mm. The effective area of water transmission through the film was 961.26 mm^2. All the assemblies were placed in desiccators at 25 °C containing small lumps of anhydrous calcium chloride. The amount of water vapours transferred through the films was measured as the mass loss of the test cup at a time interval of 1 h. Water vapour transmission rate (WVTR, g h^{-1} m^{-2}) was obtained by dividing the slope of the graph (weight loss of test cup versus time) with the area of the film (m^2). The experiment was repeated three times and average of values was reported.

2.6. Antimicrobial property

The antimicrobial activity of films was evaluated against two different pathogens: gram negative bacteria Escherichia Coli (*E. coli*, MTCC 1687) and gram positive bacteria Staphylococcus Aureus (*S. aureus*, MTCC 737) by Colony Forming Units (CFU/gm) method. The test organisms were grown in a Nutri-

Please cite this article in press as: Mujeeb Rahman, P. et al., Chitosan/nano ZnO composite films: Enhanced mechanical, antimicrobial and dielectric properties. Arabian Journal of Chemistry (2016), http://dx.doi.org/10.1016/j.arabjc.2016.09.008

ent Agar Broth media at 35–37 °C for 24 h, a period of time sufficient for the growth of microorganisms. One millilitre (mL) of culture was diluted with 99 mL of the same broth. 10 mL of this diluted media was taken separately in five different dishes having a diameter of 50 mm and previously autoclaved rectangular pieces of films (20 × 20 mm) were introduced separately into the dish. The dishes with films were shaken gently at 50 rpm at room temperature for 24 h. One milliliter of culture was taken out and diluted serially to count the number of colonies.

2.7. Dielectric properties

The dielectric properties were determined at room temperature using an impedance analyser. The impedance was measured using a fully automated instrument (HOIKY 3532-50 LCR HI-Tester). The dielectric constant and AC conductivity were calculated from the measured data using the thickness of the film.

2.8. Statistical analysis

All experiments were repeated in three times and average values with standard errors were reported. Analysis of variance was conducted and differences between variables were tested for significance by one-way ANOVA with Tukey's test using software originPro8 (Origin Lab corporation). A statistical difference at $P < 0.05$ was considered to be significant.

3. Results and discussion

3.1. FT-IR

Fig. 2a represents the FT-IR spectra of pure Chitosan. It exhibited a broadband at 3322 cm^{-1} which can be indexed to the stretching vibrations of pendant groups such as —NH_2 and —OH on the Chitosan. The band at 2872 cm^{-1} corresponds to the asymmetric stretching vibrations of —CH_2— groups of Chitosan chain. Stretching vibration of C═O and C—N groups in Chitosan is responsible for the bands at 1564 and 1370 cm^{-1}. The band obtained at 1014 cm^{-1} arises due to the stretching vibrations of —C—O—C— linkages (El. shafei and Abou-Okeil, 2011; Brugnerotto et al., 2001). It is seen the spectra of pure Chitosan showed the low intensity bands which can be attributed to insufficient contact between the film and the crystal surface (Li et al., 2010b).

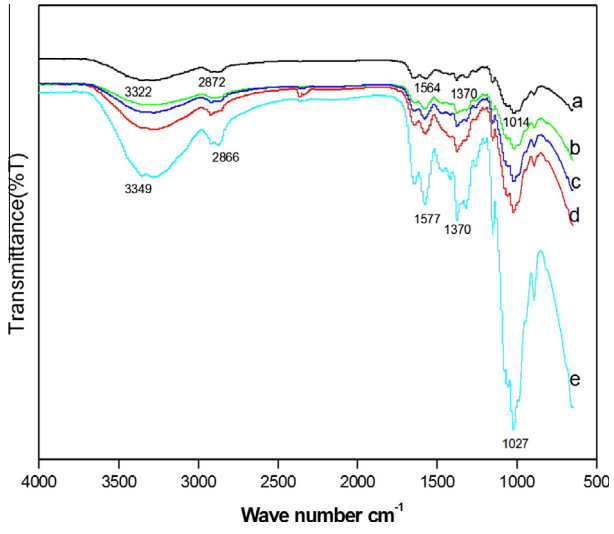

Figure 2 The IR spectra of chitosan and nano-composites films.

The IR spectra of composite films are shown in Fig. 2b–e. The incorporation of ZnO has greatly modified the IR spectra. It is evident from the spectra that the width of the bands corresponding to —NH_2 and —OH groups is inversely related to the amount of ZnO particles in the Chitosan matrix. This can be accounted by the reduction of hydrogen bonds between —NH_2 and —OH groups with the incorporation of ZnO particles onto the Chitosan matrix (Ibupoto et al., 2013). As compared to IR spectra of pure Chitosan film, considerable shift in the position of bands towards lower and higher wave number region is clearly visible in the IR spectra of composites (Table 1). This confirms stronger interaction between the functional groups and ZnO particles. The incremental increase of intensities of IR bands at 3349, 2866, 1577, 1370, 1027 cm^{-1}, is the indication of formation of coordination bonds between various groups of Chitosan and Zn^{2+} ions of nano particles; hence, it was concluded that ZnO particles will be located in between chitosan chains connecting through the functional groups (Perelshtein et al., 2013).

3.2. XRD

The XRD patterns of pure Chitosan and composite films are depicted in Fig 3. The diffraction peaks observed in the composite films at various 2θ values 33, 36, 40.35, 54.3, 61 and 71.8° can be indexed to the position of the planes of ZnO particles (002), (100), (101), (110), (103) and (201) respectively. All these data were in well agreement with the data base of ZnO particles (JCPDS No. 1436-51) (Padmavathy and Vijayaraghavan, 2008; Prabhu and Rao, 2014; Sarma and Sarma, 2014). The average particle size of ZnO crystallites was calculated using Scherrer equation, each composite film comprised of different sized nanoparticles i.e. C-0.5, C-1, C-1.5 and C-2 have particle sizes of 6.5 nm, 28.3 nm, 9.66 nm and 7.73 nm respectively. The XRD pattern of pure Chitosan exhibited a sharp peak at 20°, which can be correlated to the semicrystalline nature of Chitosan. The semicrystalline property of Chitosan arises from the compact arrangement of polymer molecules in the presence of strong inter molecular hydrogen bonds (Pawlak and Mucha, 2003). The XRD pat-

Table 1 Shift of major peaks of composite films as compared to bare chitosan film.

Sl. No	Major functional group	Wave number observed in pure chitosan film (cm^{-1})	Wave number observed in composite film (cm^{-1})
1	—NH_2 & —OH	3322	3349
2	—CH_2—	2872	2866
3	C = O	1564	1577
4	—C—O—C—	1014	1027

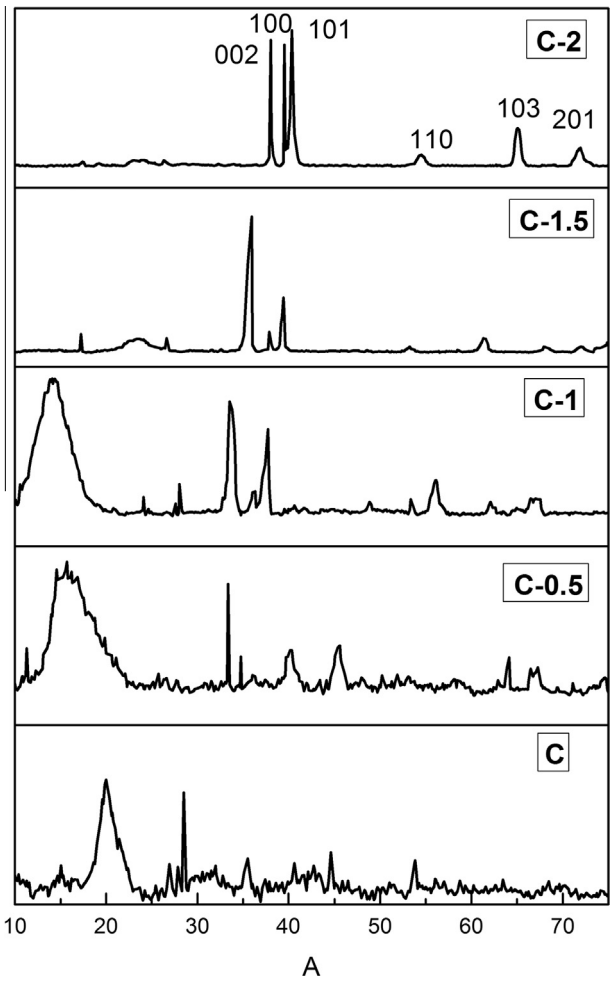

Figure 3 The XRD patterns of bare chitosan and nanocomposite films.

terns of composite films showed an interesting linear relationship between the intensities of major peaks and amount of ZnO nanoparticles. Moreover there was a notable shift in the positions of peaks. The variation of intensities and peak positions is due to the differences in size of incorporated ZnO nanoparticles and also due to the lattice strain developed in the composite because of the presence of nanoparticles (Li et al., 2010a). Hence XRD data underline the dispersion of crystalline ZnO nanoparticles on the Chitosan matrix.

3.3. Thermo gravimetric analysis

Thermal stability of films was evaluated by thermo gravimetric analysis (TGA) and results are shown in Fig. 4. Thermal properties of pure Chitosan films were already reported and well documented (Aneesh et al., 2007). As shown in the figure, all films exhibited the same thermal decomposition trend. There was no any weight loss below the 100 °C, and the slope between 100 °C and 223 °C is attributed to the loss of water molecules from the polymer films. In the case of bare Chitosan film, the significant weight loss appeared at 223 °C is correlated to the thermal degradation of polymer chains, whereas the onset of thermal degradation of composite films is observed at higher temperature 240 °C indicating enhanced thermal stability of composite films. The residual mass percentage of Chitosan and composite films was determined at 486 °C and recorded as 26%, for chitosan(C) and 36% for (C-0.5). Three other films (C-1, C-1.5 and C-2) recorded higher residual mass percentage (49%) at the same temperature. In contrast to composite films, pure Chitosan film did not show any plateau above 500 °C probably due to its complete thermal degradation above this temperature. All these data vindicate enhanced thermal stability of composite films.

3.4. SEM analysis

The surface morphology of C, C-0.5, C-1, C-1.5 and C-2 films was evaluated using scanning electron microscopy. In the SEM photographs, presence of nano ZnO particles on the polymer surface was spotted as white coloured images. As shown in Fig. 5a, the surface of pure Chitosan film is rather smooth, compact and homogenous, whereas in composite films (Fig. 5b–d) the incorporation of nanoparticles modified the Chitosan surface to coarse and heterogeneous. In the SEM images of composite films, agglomeration of nanoparticles was observed and the mode of distribution of nanoparticles was different in different films. The image of C-1 film exhibited the distribution of equal sized clusters of particles throughout the surface but high degree of agglomeration of nanoparticles was observed in C-2 films. These nanoparticles were strongly adhered to the chitosan matrix and modified physical and chemical features of chitosan.

3.5. Mechanical properties measurement

The wide range of applicability of any film as a packaging material is significantly pertained to its mechanical properties such as tensile strength and elongation at break. According to previous reports, mechanical properties of Chitosan based films are affected by different factors such as degrees of deacetylation, molecular weight, amount of chitosan and fillers (Devlieghere et al., 2004; Zuo et al., 2013).

The fashion of change of tensile strength (TS) and elongation at break (EB) is given in Table 2. Bare chitosan film exhibited TS and EB values of 12.84 ± 0.62 MPa and 30.42 ± 0.95% respectively. The variation of tensile strength of composite films with the amount of ZnO particles is quite different. The values of TS increased initially, attained a maximum value at C-1 film and set to decrease. Yet all composite films maintained higher TS values as compared to bare Chitosan films. The enhancement of TS of composite films is explained as follows. When nano ZnO particles are incorporated, they exist in between polymer chains and an intermolecular cross linking effect is generated. This observation is inconsistent with FTIR and SEM analysis.

In the case of EB, when nano ZnO particles are incorporated a reverse trend was observed except in C-1. The EB values sharply lowered from 30.42 ± 0.95% in C to 13.36 ± 0.69% in C-2. But C-1 has showcased anomalously higher EB value 32.44 ± 0.52 indicating its distinctive mechanical feature. The characteristic mechanical property of C-1 was again justified by its unique WVTR values and a similar trend was also observed in Chitosan/lignin composite film (Chen et al., 2009).

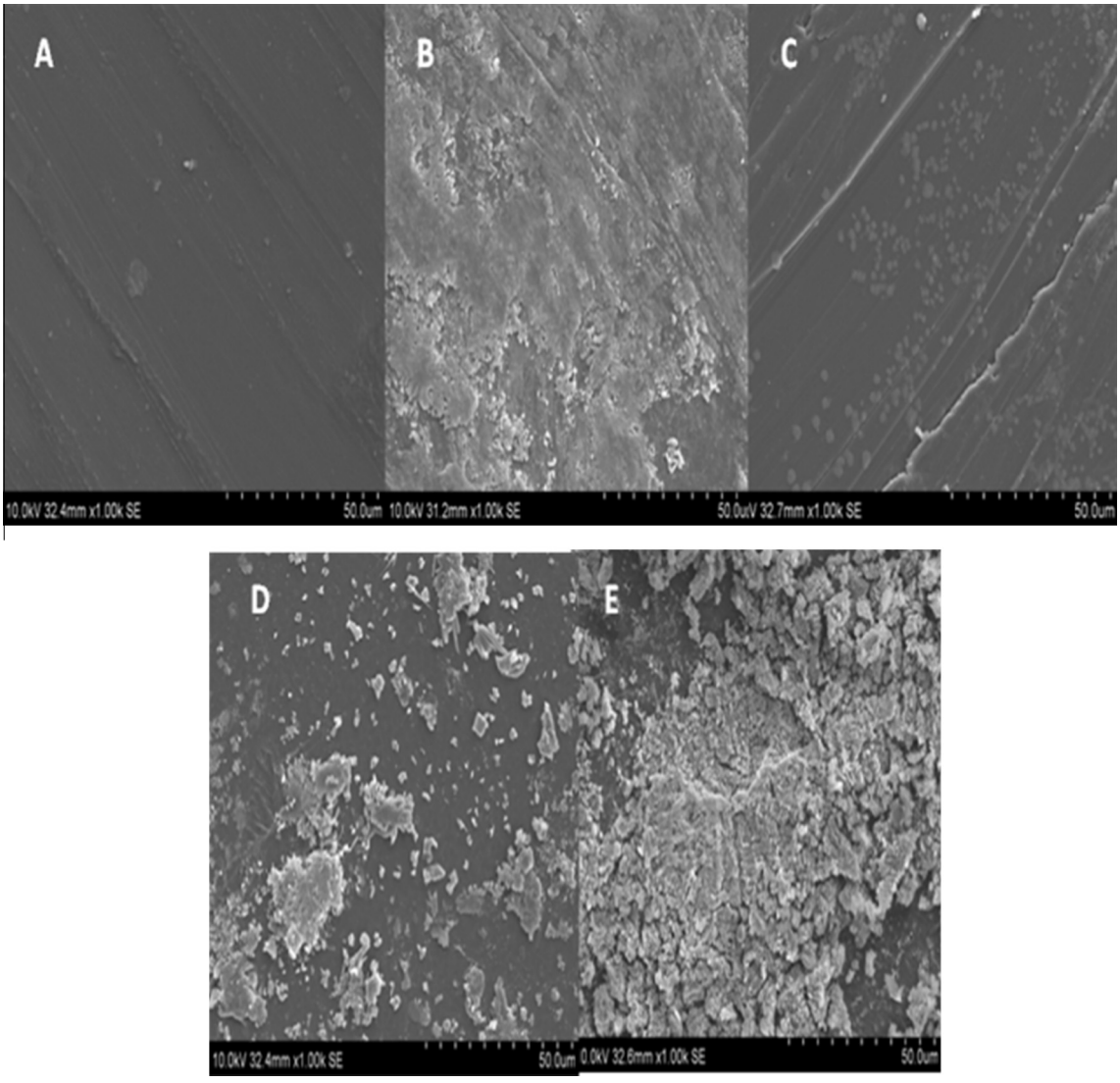

Figure 4 SEM images of (A) pure chitosan film, (B) C-0.5 film, (C) C-1 film, (D) C-1.5 film and (E) C-2film.

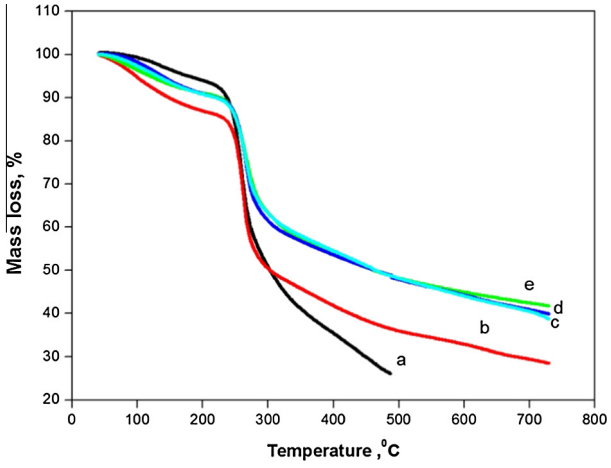

Figure 5 TGA analysis bare chitosan film (a), C-0.5 (b), C-1 (c), C-1.5 (d) and C-2 (e).

3.6. Water vapour transmission rate

Water vapour transmission rate (WVTR) is the measure of ease of moistures to penetrate and cross any film, which is an important property to be accounted for packaging applications. Excess water molecules inside the pack will lead to undesirable changes in foods, whereas moderate amount of water molecules is tolerable to transfer active molecules from the packaging films to the food surface. Hence, depending upon food and mechanisms involved in enhancement of its shelf life, the specificity of WVTR of a packaging film will be changed. The values of WVTR are given in Table 3. As shown in the result, all composite films exhibited lower WVTR values compared to bare Chitosan film except C-1. It is found that WVTR of films was inversely related to the amount of ZnO particles. When nano ZnO particles are incorporated in chitosan matrix, segmental motion and porosity in the polymer surface are reduced leading to low water vapour transmission. The exceptionality of C-1 film is attributed to its unique feature as revealed by mechanical property analysis.

Table 2 Mechanical properties of films.

Sample	Tensile strength (MPa)	Elongation at break (%)
C	12.84 ± 0.62[a]	30.42 ± 0.95[a]
C-0.5	26.1 ± 0.96[b]	22.62 ± 0.577[b]
C-1	41.73 ± 0.48[c]	32.44 ± 0.52[c]
C-1.5	36.21 ± 0.28[d]	14.71 ± 0.37[d]
C-2	28.55 ± 1.28[e]	13.36 ± 0.69[e]

Each value indicates means of three set of samples at identical conditions.
Superscript letters (a–e) within the column indicate significant differences between mean values ($P < 0.05$).

3.7. Dielectric property

Dielectric property is the very less exploited feature of Chitosan nano metal oxide composite films. The dielectric property of flexible Chitosan composite materials is technologically inspiring due to many reasons such as cost effectiveness, biocompatibility and processability. It will find applications in new generation actuators, sensors, fuel cells, capacitors and self regulating heaters. Flexible biocompatible films with tunable dielectric property can act as artificial muscle in future medical treatment and are expected to have a major role in the realization of 'smart skins' in medical field (Chiang and Popielarz, 2002; Devi and Ramachandran, 2011; Kondawar et al., 2014; Marroquin et al., 2013). The dielectric property of Chitosan composite materials depends on various complex factors and it is unexploited. There are only a few reports on dielectric properties of certain synthetic polymer composites (Qureshi et al., 2008).

The percolation theory is commonly used to explain the dielectric property of polymer composites. According to this theory, gradual addition of metal oxides onto the polymer matrix increases its dielectric values. At a critical amount, a swift in dielectric value will be shown and it is designated as percolation threshold (Pc). The amount of a substance corresponding to this sharp change in dielectric value is considered as percolation value (Zois et al., 2003). In the present case, all composite films exhibited higher dielectric values compared to bare Chitosan film (Fig. 6). The enhancement of dielectric properties of composite films is assigned to development of different types of polarizations in composite films. The interfaces of composite materials contain large numbers of defects, which result the unequal charge distributions and pave the way to space charge polarizations when an electric field is applied. When the amount of ZnO particles increases, space polarization also increases in the interface of composite materials leading to enhancement of dielectric values. The continuous decrease of dielectric constant with an increase in frequency is quite common for all dielectric substances. It is well known that, when frequency of electric field is increased the mechanism of polarization cannot be able to follow the change in the electric field and therefore, the contribution of polarization to the dielectric constant will be lowered (Moretro and Daeschel, 2004).

The conductivity values of composite films were compared to those of pure chitosan film (Fig. 7). The C-2 film exhibited highest conductivity, whereas pure Chitosan film displayed lowest values of conductivities in all frequencies. The variation of conductivities of bare Chitosan film at different frequencies was negligible but significant changes are shown by the composite films. The smart conductivity exhibited by C-2 films at all frequencies justifies the development of smooth conduction pathway in the presence of nanoparticles. In C2, as shown in its SEM images, a compact and connected array of semiconducting ZnO particles are framed in the polymer matrix leading to continuous carrier way or tunnelling for charges in the composite film (Sharma et al., 2012).

Table 3 Water vapour transmission rate of films.

Sample	WVTR (g/h m^2)
C	22.2 ± 0.67[a]
C-0.5	21.7 ± 0.41[b]
C-1	22.53 ± 0.31[c]
C-1.5	21.63 ± 0.11[d]
C-2	20.57 ± 0.17[e]

Each value indicates means of three set of samples at identical conditions.
Superscript letters (a–e) within the column indicate significant differences between mean values ($P < 0.05$).

3.8. Anti microbial property

The antimicrobial activity of bare chitosan and against *S. aureus* and *E. coli* was investigated by colony counting method. The results of study are given in Table 4. Control Chitosan did not show any appreciable antimicrobial activity towards both strains when compared to composite films. The investigation also revealed that the antimicrobial activity is linearly related to the amount of nano ZnO particles in the composite films. Hence C-2 is the most efficient composite film against both *E. coli* and *S. aureus*. All results hint to the fact that the commendable antimicrobial activity of the composite relays on the presence of nano ZnO particles in the matrix. It is believed that the ZnO nano particles release reactive oxygen species (ROS). The ROS together with Zn^{2+} ions attack the negatively charged cell wall and will lead to leakage and ultimately in death of bacteria (Zhang and Xiong, 2015).

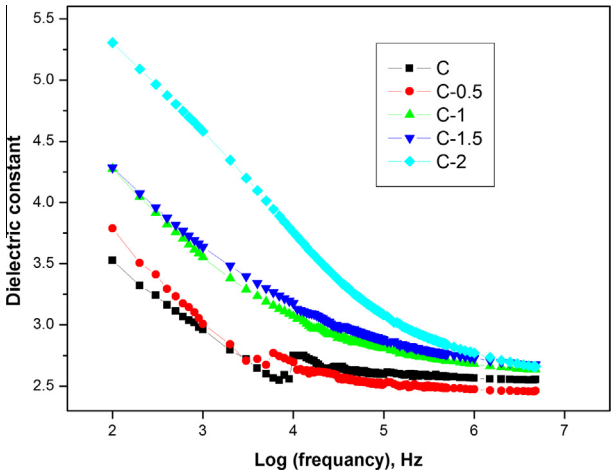

Figure 6 Variation of dielectric constant of films with frequency.

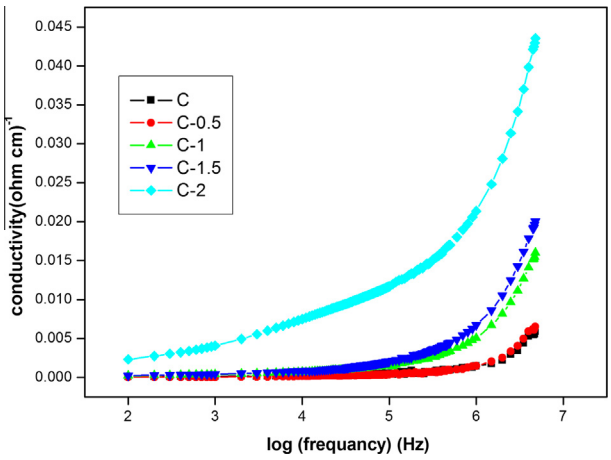

Figure 7 Variation of conductivity of films with frequency.

Table 4 Plate count (cfu/g) values of films against two bacteria (*E. coli*, MTCC 1687) and (*S. aureus*, MTCC 737).

Sl. No	Sample	*E. coli* (cfu/g)	*S. aureus* (cfu/g)
1	C	$9.5 \pm 0.336^{a} \times 10^{9}$	$10.4 \pm 0.303^{a} \times 10^{9}$
2	C-0.5	$5 \pm 0.421^{b} \times 10^{9}$	$6.3 \pm 0.378^{b} \times 10^{9}$
3	C-1	$4 \pm 0.298^{c} \times 10^{9}$	$5 \pm 0.301^{c} \times 10^{9}$
4	C-1.5	$2.4 \pm 0.315^{a} \times 10^{9}$	$3.5 \pm 0.273^{a} \times 10^{9}$
5	C-2	$2.5 \pm 0.421^{d,e} \times 10^{7}$	$9 \pm 0.367^{d,e} \times 10^{7}$

Each value indicates means of three set of samples at identical conditions.
Same superscript letter indicates no significant differences between mean values ($P > 0.05$).
[e] C-2 sample was serially diluted for seven times only due to its high antimicrobial activity.

Moreover, the addition of ZnO, enhances the positive charge on the amino group of chitosan. This results in easier interaction with anionic components on cell wall and composite films. The decreased activity of all kinds of composites towards *S. aureus* bacteria is due to the presence of thick layer of peptide glycans in its cell wall (Leceta et al., 2013; Sudheesh Kumar et al., 2012).

4. Conclusions

Four different Chitosan/nano ZnO composite films were synthesized; their physical, mechanical, antimicrobial and dielectric properties of all composite films were evaluated. The mechanical property measurement showcased an enhancement of Tensile strength in the presence of nano ZnO particles. The antimicrobial efficacy of the composite films was significantly improved when nanoparticles were incorporated and C-2 film exhibited highest inhibition efficiency. Enhancement of dielectric constant and conductivity of films were observed when nano ZnO particles were incorporated. Moreover, these properties were linearly related to the amount of nanoparticles. These results justify that the prepared novel Chitosan/nano ZnO composite films will be an elite entrant in area of bionanocomposites.

References

Aneesh, P.M., Vanaja, K.A., Jayaraj, M.K., 2007. Synthesis of ZnO Nanoparticles by Hydrothermal Method 66390J–66390J–9. http://dx.doi.org/10.1117/12.730364.

Bourtoom, T., Chinnan, M.S., 2008. Preparation and properties of rice starch–chitosan blend biodegradable film. LWT – Food Sci. Technol. 41, 1633–1641. http://dx.doi.org/10.1016/j.lwt.2007.10.014.

Brugnerotto, J., Lizardi, J., Goycoolea, F.M., Argüelles-Monal, W., Desbrières, J., Rinaudo, M., 2001. An infrared investigation in relation with chitin and chitosan characterization. Polymer (Guildf) 42, 3569–3580. http://dx.doi.org/10.1016/S0032-3861(00)00713-8.

Chen, J.Y., Zhou, P.J., Li, J.L., Wang, Y., 2008. Studies on the photocatalytic performance of cuprous oxide/chitosan nanocomposites activated by visible light. Carbohydr. Polym. 72, 128–132. http://dx.doi.org/10.1016/j.carbpol.2007.07.036.

Chen, L., Tang, C., Ning, N., Wang, C., Fu, Q., Zhang, Q., 2009. Preparation and properties of chitosan/lignin composite films. Chinese J. Polym. Sci. 27, 739–746. http://dx.doi.org/10.1142/S0256767909004448.

Chiang, C.K., Popielarz, R., 2002. Polymer composites with high dielectric constant. Ferroelectrics 275, 1–9. http://dx.doi.org/10.1080/00150190214285.

Dehnad, D., Mirzaei, H., Emam-Djomeh, Z., Jafari, S.-M., Dadashi, S., 2014. Thermal and antimicrobial properties of chitosan–nanocellulose films for extending shelf life of ground meat. Carbohydr. Polym. 109, 148–154. http://dx.doi.org/10.1016/j.carbpol.2014.03.063.

Devi, P.I., Ramachandran, K., 2011. Dielectric studies on hybridised PVDF–ZnO nanocomposites. J. Exp. Nanosci. 6, 281–293. http://dx.doi.org/10.1080/17458080.2010.497947.

Devlieghere, F., Vermeulen, a., Debevere, J., 2004. Chitosan: antimicrobial activity, interactions with food components and applicability as a coating on fruit and vegetables. Food Microbiol. 21, 703–714. http://dx.doi.org/10.1016/j.fm.2004.02.008.

Dutta, P.K., Tripathi, S., Mehrotra, G.K., Dutta, J., 2009. Perspectives for chitosan based antimicrobial films in food applications. Food Chem. 114, 1173–1182. http://dx.doi.org/10.1016/j.foodchem.2008.11.047.

El.shafei, A., Abou-Okeil, A., 2011. ZnO/carboxymethyl chitosan bionano-composite to impart antibacterial and UV protection for cotton fabric. Carbohydr. Polym. 83, 920–925. http://dx.doi.org/10.1016/j.carbpol.2010.08.083.

Ibupoto, Z., Khun, K., Eriksson, M., AlSalhi, M., Atif, M., Ansari, A., Willander, M., 2013. Hydrothermal growth of vertically aligned ZnO nanorods using a biocomposite seed layer of ZnO nanoparticles. Materials (Basel) 6, 3584–3597. http://dx.doi.org/10.3390/ma6083584.

Jiang, R., Zhu, H., Li, X., Xiao, L., 2009. Visible light photocatalytic decolourization of C.I. Acid Red 66 by chitosan capped CdS composite nanoparticles. Chem. Eng. J. 152, 537–542. http://dx.doi.org/10.1016/j.cej.2009.05.037.

Jiang, R., Zhu, H., Yao, J., Fu, Y., Guan, Y., 2012. Chitosan hydrogel films as a template for mild biosynthesis of CdS quantum dots with highly efficient photocatalytic activity. Appl. Surf. Sci. 258, 3513–3518. http://dx.doi.org/10.1016/j.apsusc.2011.11.105.

Kondawar, S.B., Dahegaonkar, A.D., Tabhane, V.A., Nandanwar, D. V., 2014. Thermal and frequency dependance dielectric properties of conducting polymer/fly ash composites. Adv. Mat. Lett. 5, 360–365. http://dx.doi.org/10.5185/amlett.2014.amwc.1036.

Leceta, I., Guerrero, P., Ibarburu, I., Dueñas, M.T., de la Caba, K., 2013. Characterization and antimicrobial analysis of chitosan-based films. J. Food Eng. 116, 889–899. http://dx.doi.org/10.1016/j.jfoodeng.2013.01.022.

Li, L.-H., Deng, J.-C., Deng, H.-R., Liu, Z.-L., Xin, L., 2010a. Synthesis and characterization of chitosan/ZnO nanoparticle composite membranes. Carbohydr. Res. 345, 994–998. http://dx.doi.org/10.1016/j.carres.2010.03.019.

Li, Y., Wu, K., Zhitomirsky, I., 2010b. Electrodeposition of composite zinc oxide-chitosan films. Colloids Surfaces A Physicochem. Eng. Asp. 356, 63–70. http://dx.doi.org/10.1016/j.colsurfa.2009.12.037.

Marroquin, J.B., Rhee, K.Y., Park, S.J., 2013. Chitosan nanocomposite films: enhanced electrical conductivity, thermal stability, and mechanical properties. Carbohydr. Polym. 92, 1783–1791. http://dx.doi.org/10.1016/j.carbpol.2012.11.042.

Martínez-Camacho, a.P., Cortez-Rocha, M.O., Ezquerra-Brauer, J. M., Graciano-Verdugo, a.Z., Rodriguez-Félix, F., Castillo-Ortega, M.M., Yépiz-Gómez, M.S., Plascencia-Jatomea, M., 2010. Chitosan composite films: thermal, structural, mechanical and antifungal properties. Carbohydr. Polym. 82, 305–315. http://dx.doi.org/10.1016/j.carbpol.2010.04.069.

Moretro, T., Daeschel, M., 2004. Wine is bactericidal to foodborne pathogens. J. Food Sci. 69, 251–257. http://dx.doi.org/10.1111/j.1365-2621.2004.tb09938.x.

Padmavathy, N., Vijayaraghavan, R., 2008. Enhanced bioactivity of ZnO nanoparticles—an antimicrobial study. Sci. Technol. Adv. Mater. 9, 035004. http://dx.doi.org/10.1088/1468-6996/9/3/035004.

Pawlak, a., Mucha, M., 2003. Thermogravimetric and FTIR studies of chitosan blends. Thermochim. Acta 396, 153–166. http://dx.doi.org/10.1016/S0040-6031(02)00523-3.

Perelshtein, I., Ruderman, E., Perkas, N., Tzanov, T., Beddow, J., Joyce, E., Mason, T.J., Blanes, M., Mollá, K., Patlolla, A., Frenkel, A.I., Gedanken, A., 2013. Chitosan and chitosan–ZnO-based complex nanoparticles: formation, characterization, and antibacterial activity. J. Mater. Chem. B 1, 1968. http://dx.doi.org/10.1039/c3tb00555k.

Prabhu, Y.T., Rao, K.V., 2014. X-ray analysis by Williamson-Hall and size-strain plot methods of ZnO nanoparticles with fuel variation. World J. Nano Sci. Eng. 4, 21–28. http://dx.doi.org/10.4236/wjnse.2014.41004.

Qureshi, A., Mergen, A., Eroğlu, M.S., Singh, N.L., Güllüoğlu, A., 2008. Dielectric properties of polymer composites filled with different metals. J. Macromol. Sci. Part A 45, 462–469. http://dx.doi.org/10.1080/10601320801977756.

Salehi, R., Arami, M., Mahmoodi, N.M., Bahrami, H., Khorramfar, S., 2010. Novel biocompatible composite (Chitosan–zinc oxide nanoparticle): preparation, characterization and dye adsorption properties. Colloids Surfaces B Biointerfaces 80, 86–93. http://dx.doi.org/10.1016/j.colsurfb.2010.05.039.

Sarma, H., Sarma, K.C., 2014. X-ray peak broadening analysis of ZnO nanoparticles derived by precipitation method. IJSRP 4, 1–7.

Sharma, S., Sanpui, P., Chattopadhyay, A., Ghosh, S.S., 2012. Fabrication of antibacterial silver nanoparticle—sodium alginate–chitosan composite films. RSC Adv. 2, 5837. http://dx.doi.org/10.1039/c2ra00006g.

Sudheesh Kumar, P.T., Lakshmanan, V.-K., Anilkumar, T.V., Ramya, C., Reshmi, P., Unnikrishnan, a.G., Nair, S.V., Jayakumar, R., 2012. Flexible and microporous chitosan hydrogel/nano ZnO composite bandages for wound dressing: in vitro and in vivo evaluation. ACS Appl. Mater. Interfaces 4, 2618–2629. http://dx.doi.org/10.1021/am300292v.

Tripathi, S., Mehrotra, G.K., Dutta, P.K., 2011. Chitosan-silver oxide nanocomposite film: preparation and antimicrobial activity. Bull. Mater. Sci. 34, 29–35. http://dx.doi.org/10.1007/s12034-011-0032-5.

Xu, Y.X., Kim, K.M., Hanna, M.a., Nag, D., 2005. Chitosan–starch composite film: preparation and characterization. Ind. Crops Prod. 21, 185–192. http://dx.doi.org/10.1016/j.indcrop.2004.03.002.

Yan, E., Wang, C., Wang, S., Sun, L., Wang, Y., Fan, L., Zhang, D., 2011. Synthesis and characterization of fluorescent chitosan-ZnO hybrid nanospheres. Mater. Sci. Eng., B 176, 458–461. http://dx.doi.org/10.1016/j.mseb.2011.01.005.

Zhang, W., Yang, T., Huang, D.M., Jiao, K., 2008. Electrochemical sensing of DNA immobilization and hybridization based on carbon nanotubes/nano zinc oxide/chitosan composite film. Chinese Chem. Lett. 19, 589–591. http://dx.doi.org/10.1016/j.cclet.2008.03.012.

Zhang, Z.-Y., Xiong, H.-M., 2015. Photoluminescent ZnO nanoparticles and their biological applications. Materials (Basel) 8, 3101–3127. http://dx.doi.org/10.3390/ma8063101.

Zhu, H., Jiang, R., Xiao, L., Chang, Y., Guan, Y., Li, X., Zeng, G., 2009. Photocatalytic decolorization and degradation of Congo Red on innovative crosslinked chitosan/nano-CdS composite catalyst under visible light irradiation. J. Hazard. Mater. 169, 933–940. http://dx.doi.org/10.1016/j.jhazmat.2009.04.037.

Zois, H., Apekis, L., Mamunya, Y.P., 2003. Dielectric permittivity and morphology of polymer composites filled with dispersed iron. J. Appl. Polym. Sci. 88, 3013–3020. http://dx.doi.org/10.1002/app.12118.

Zuo, P., Feng, H., Xu, Z., Zhang, L., Zhang, Y., Xia, W., Zhang, W., 2013. Fabrication of biocompatible and mechanically reinforced graphene oxide-chitosan nanocomposite films. Chem. Cent. J., 1–11 http://dx.doi.org/10.1186/1752-153X-7-39.

Please cite this article in press as: Mujeeb Rahman, P. et al., Chitosan/nano ZnO composite films: Enhanced mechanical, antimicrobial and dielectric properties. Arabian Journal of Chemistry (2016), http://dx.doi.org/10.1016/j.arabjc.2016.09.008